CORTEX 149 (2022) 85–100

Available online at www.sciencedirect.com

ScienceDirect

Journal homepage: www.elsevier.com/locate/cortex

Research Report

ASMR amplifies low frequency and reduces high frequency oscillations

Thomas R. Swart [a,*], Michael J. Banissy [a,b], Thomas P. Hein [a], Ricardo Bruña [c,d,e], Ernesto Pereda [c,e] and Joydeep Bhattacharya [a]

[a] Department of Psychology, Goldsmiths, University of London, United Kingdom
[b] School of Psychological Science, University of Bristol, United Kingdom
[c] Laboratory of Cognitive and Computational Neuroscience (Center for Biomedical Technology), Universidad Politécnica de Madrid y Universidad Complutense de Madrid, Spain
[d] Networking Research Center on Bioengineering, Biomaterials and Nanomedicine (CIBER-BBN), Madrid, Spain
[e] Department of Industrial Engineering & IUNE & ITB, University of La Laguna, San Cristóbal de La Laguna, Spain

ARTICLE INFO

Article history:
Received 23 August 2021
Reviewed 5 October 2021
Revised 26 November 2021
Accepted 10 January 2022
Action editor Ryo Kitada
Published online 2 February 2022

Keywords:
ASMR
Autonomous sensory meridian response
EEG
Beamformer
Source reconstruction

ABSTRACT

Autonomous sensory meridian response (ASMR) describes an atypical multisensory experience of calming, tingling sensations in response to a specific subset of social audiovisual triggers. To date, the electrophysiological (EEG) correlates of ASMR remain largely unexplored. Here we sought to provide source-level signatures of oscillatory changes induced by this phenomenon and investigate potential decay effects—oscillatory changes in the absence of self-reported ASMR. We recorded brain activity using EEG as participants watched ASMR-inducing videos and self-reported changes in their state: no change (Baseline); enhanced relaxation (Relaxed); and ASMR sensations (ASMR). Statistical tests in the sensor-space were used to inform contrasts in the source-space, executed with beamformer reconstruction. ASMR modulated oscillatory power by decreasing high gamma (52–80 Hz) relative to Relaxed and by increasing alpha (8–13 Hz) and decreasing delta (1–4 Hz) relative to Baseline. At the source level, ASMR increased power in the low-mid frequency ranges (8–18 Hz) and decreased power in high frequency (21–80 Hz). ASMR decay effects reduced gamma (30–80 Hz) and in the source-space reduced high-beta/gamma power (21–80 Hz). The temporal profile of ASMR modulations in high-frequency power later shifts to lower frequencies (1–8 Hz), except for an enhanced alpha, which persists for up to 45 min post self-reported ASMR. Crucially, these results provide the first evidence that the cortical sources of ASMR tingling sensations may arise from decreases in higher frequency oscillations and that ASMR may induce a sustained relaxation state.

* *Corresponding author*. Department of Psychology, Department of Psychology, Goldsmiths, University of London, New Cross, London SE14 6NW, UK.
E-mail address: tswar001@gold.ac.uk (T.R. Swart).
https://doi.org/10.1016/j.cortex.2022.01.004

1. Introduction

People who experience Autonomous Sensory Meridian Response (ASMR) report calming and pleasant tingling sensations that originate in the crown of the head when encountering specific audio-visual triggers (Barratt & Davis, 2015). Typically these tingling sensations originate at the back of the head and neck; they are then thought to radiate down the spine and into the limbs in periods of greater intensity (Barratt & Davis, 2015). ASMR induction is thought to be involuntary and heavily dependent on the environment and individual mood (Barratt & Davis, 2015; Poerio et al., 2018). Anecdotal evidence suggests individuals watch ASMR-eliciting stimuli to relieve symptoms of stress, anxiety, or even chronic pain (Barratt & Davis, 2015). However, the therapeutic benefits of ASMR and the prevalence of ASMR-Responders (individuals capable of experiencing ASMR) in the general population are currently unknown.

Stimuli known to induce ASMR are idiosyncratic and thus can vary enormously. However, certain features are common (Barratt & Davis, 2015), including low volume voices (e.g., soft-spoken, whispering), repetitive movements or sounds (e.g., tapping, scratching, brushing), layered sounds, personal attention, close-up visuals, and expert manipulation of objects (Barratt et al., 2017; Barratt & Davis, 2015; Fredborg et al., 2017, 2018). In addition, there is further anecdotal evidence that touch is a strong trigger (Kovacevich & Huron, 2019; Poerio et al., 2018).

Some studies provide evidence of physiological correlates of ASMR. For instance, altered heart rate and skin conductance responses have been shown when viewing ASMR videos in ASMR-Responders versus non-Responders (Poerio et al., 2018). However, no data has yet to be published regarding heart rate variability. In addition, there are several task-based and resting-state fMRI studies in ASMR (Smith et al., 2017; 2019a; 2019b, 2020). In these studies, reduced functional connectivity of resting states was found in ASMR-Responders compared to non-Responders (Smith et al., 2017). Specifically, ASMR-Responders showed reduced functional connectivity in the right precuneus and posterior cingulate, the left medial frontal gyrus and thalamus, and bilateral superior temporal gyri. Conversely, increased functional connectivity was observed in the right occipital and left frontal cortical areas. The authors suggested that this could indicate a reduced ability to suppress multisensory experiences in these individuals.

In a task-based fMRI where 34 participants (17 ASMR-Responders and 17 non-Responders) watched ASMR stimuli and control stimuli, differential activation of regions was shown through group comparisons (Smith et al., 2019b). Specifically, episodes of ASMR were associated with increased activity in medial prefrontal regions, bilateral precentral gyri, the right superior prefrontal cortex, the left superior temporal cortex, and midline occipito-parietal structures (precuneus and cuneus). In contrast, control participants showed only a decrease in activity in the cuneus (Smith et al., 2019b).

Another fMRI study investigated ASMR-induced changes relative to an individual baseline within ASMR-Responders (Lochte et al., 2018). Ten participants reported three states: no change (i.e., Baseline), Relaxation, or ASMR (e.g., the tingling sensations). When Relaxation was compared to Baseline, there was increased activity in the medial prefrontal cortex. When ASMR was compared to Baseline, there was increased activity in the media prefrontal cortex, bilateral nucleus accumbens, bilateral insula/inferior frontal gyrus, ventral premotor cortex, dorsal anterior cingulate cortex, left inferior parietal lobule, bilateral supplementary motor area and the left secondary somatosensory cortex. Reassuringly, the processes associated with these regions, such as reward responses (e.g., see review Schultz, 2000), interoception (e.g., see review Craig & Craig, 2009), and emotional arousal (e.g., Oliveri et al., 2003), were all implicated, thus supporting the reported phenomenology of ASMR (Barratt & Davis, 2015).

Another investigatory tool to study the neural correlates of ASMR spontaneous EEG, for example, the time-frequency oscillations derived from the electrophysiological data. Using such oscillatory neuroelectric activity, researchers can estimate the degree of involvement and synchrony that neurons exhibit when undergoing a specific cognitive function (e.g., Başar et al., 1999). These oscillations vary in frequency (rate of neuronal activity) and location, and can be associated with a context-specific process. For example, alpha waves (8–13 Hz) has been associated with relaxation (Niedermeyer, 1999) or the suppression of distractor stimuli (Foxe & Snyder, 2011; Jensen et al., 2002; Kelly, Lalor, Reilly, & Foxe, 2006).

Recently, researchers have published an EEG study investigating the oscillatory changes induced by ASMR in the sensor space (Fredborg et al., 2021). In this EEG ASMR study, 28 participants (14 ASMR-Responders, 14 matched non-Responders) indicated the presence of ASMR tingling sensations with a button press whilst presented with audio/audiovisual ASMR stimuli or audio/audiovisual control stimuli. Oscillatory power was estimated 500–1000 ms after button press (ASMR onset) contrasted against 500–1000 ms before button press (Baseline) in the alpha (8–12 Hz), sensorimotor rhythm (12.5–15 Hz), theta (4–7 Hz), and gamma (>30Hz) frequency bands. A between-group contrast revealed significantly enhanced alpha power at frontal, parietal, and precuneus electrodes for the audio ASMR trials. Only the enhanced alpha precuneus effect was replicated for the audiovisual contrast. Exploratory analysis for the audio trials also revealed significantly enhanced alpha power at occipital, parietal, and temporal regions in ASMR-Responders compared to non-Responders. Moreover, an enhancement of gamma power was seen at central electrodes for the audio trials only. An increase in sensorimotor rhythm power was seen at sensorimotor regions (C3, Cz, C4) for ASMR-Responders during audio trials.

Within-subjects contrasts of ASMR-inducing stimuli against control stimuli in the audio trials revealed a similar significant enhancement of alpha power in frontal and cuneus electrodes. Exploratory analysis for the audio trials also revealed enhanced alpha at P3 and P4 for ASMR-Responders only.

Baseline within-subjects contrasts of audio trials in ASMR-Responders revealed enhancements of alpha power in frontal and medial frontal regions. Conversely, the same contrasts in non-Responders (using the times from the matched ASMR-Responders) reported decreases in alpha power in frontal, medial frontal, and precuneus regions. Exploratory analysis

for ASMR-Responders during ASMR audio trials revealed significant alpha power enhancement at frontal and frontocentral electrodes. Furthermore, sensorimotor rhythm power increased for ASMR-Responders in audio trials only, whilst decreased for non-Responders.

This study has provided an excellent foundation for further EEG investigation into ASMR using time-frequency techniques. However, the authors acknowledge limitations, primarily the small sample size per group. We aim to address these gaps and build on prior work. Given the large effect sizes for alpha power enhancement seen in the previous EEG paper (e.g., $g = 1.79$; Fredborg et al., 2021), we expect to replicate this finding foremost. This prediction is further supported by the association of alpha power with distraction suppression (e.g., Jensen et al., 2002), where ASMR has previously been described as a trance-like state (Barratt & Davis, 2015). We also aim to identify: 1) oscillatory neural correlates of ASMR during the tingling experience in both the sensor and source space; 2) decay effects of ASMR after the tingling sensations have ceased and estimate possible durations of such; and 3) identify the importance of temporal continuity of ASMR stimuli for ASMR induction through a novel control stimuli design.

2. Methods and materials

We report how we determined our sample size, all data exclusions (if any), all inclusion/exclusion criteria, whether inclusion/exclusion criteria were established prior to data analysis, all manipulations, and all measures in the study.

2.1. Participants

Twenty-six healthy individuals (22 right-handed, 15 female, aged 18–45 years, mean ± SD: 27.0 ± 1.4 years) took part in this study. Resting state data from one participant could not be recorded. Participants were recruited via mailing lists at Goldsmiths University, social media platforms (e.g., reddit.com/r/ASMR), and word of mouth. All participants reported normal auditory, normal or corrected-to-normal visual acuity, and no neurological or psychiatric problems. All participants were classified as either weak or strong ASMR-Responders using the data-driven tool ASMR-Experience Questionnaire (Swart et al., 2021; freely available at https://osf.io/pazr5/). The study protocol was approved by the ethics committee of the Department of Psychology at the Goldsmiths University of London. All participants gave written informed consent before the study and were remunerated with either £20 or equivalent course credits. At the time of testing, no prior studies on ASMR using EEG had been conducted to help motivate our sample size. Accordingly, we followed an EEG study on similar phenomena (such as frisson) to inform our sample size (Trochidis & Bigand, 2012). Since completing our study, one EEG study investigating ASMR has been published, finding effects when testing fourteen participants (Fredborg et al., 2021).

2.2. Materials

To maximise the likelihood of ASMR, participants provided a 10 min long individualised ASMR video for the experiment. Since there is anecdotal evidence for a habituated ASMR response upon repeated exposure to the same ASMR video called ASMR tolerance, we requested that the individualised video be relatively new to the participant. To construct control videos, we randomly segmented each video in 120 5-sec segments and re-ordered them using *ffmpeg* (an open-source multimedia editing tool https://ffmpeg.org/)—ensuring the low-level spatial and acoustic features were preserved between experimental and control videos.

2.3. Experimental design

Each participant watched their chosen ASMR video, once scrambled (as control) and once in its original form (as experimental). Participants were seated approximately 50 cm in front of a computer screen in a dimly lit, sound-attenuated room whilst using in-ear earphones. First, 5 min of resting-state EEG with eyes closed was recorded, followed by 5 min of resting-state EEG with eyes open (fixating on a cross presented in the middle of the screen, see Fig. 1). While watching the ASMR videos, the participant was instructed to keep their eyes open and press one of four buttons as frequently as they needed to indicate a change to their subjective state. The experimental design thus furnished four subjective self-reported states in each participant, formally defined as i) an unchanged normal state (Baseline), ii) a relaxed state with no tingling (Relaxed), iii) a state characterised by weak tingling sensation (WeakASMR), and iv) a state characterised by strong tingling sensations (StrongASMR). A button press was also mandatory at the beginning of each video.

The order of the control and the experimental ASMR videos were counterbalanced between participants, and each video was separated by 2 min of rest with a fixation cross presented on the screen (Fig. 1).

2.4. Electrophysiology acquisition

EEG signals were recorded with sixty-four Ag–AgCl electrodes (placed in accordance to the extended 10–20 system; Oostenveld & Praamstra, 2001) using the BioSemi ActiveTwo head cap and the ActiveTwo BioSemi system amplifier (BioSemi, Amsterdam, The Netherlands). The EEG signal was amplified by a BioSemi ActiveTwo amplifier and sampled at 512 Hz. Four external electrodes were placed above and below each eye and at the outer canthus of each eye—to record vertical (VEOG) and horizontal eye movements (HEOG), respectively. In addition, two external electrodes were placed on both ear lobes of each participant for re-referencing. Two additional electrodes were placed below the left clavicle and above the right hip bone to record ECG.

EEG data were preprocessed in MATLAB (MathWorks, Natick, MA) using the EEGLAB v2019.1 toolbox (Delorme & Makeig, 2004). Next, further data and statistical analysis were performed using the FieldTrip toolbox (Oostenveld et al., 2011). First, we re-referenced the data to the arithmetic average of the two earlobes. After, high-pass filtered was performed at .5 Hz (Hamming windowed finite impulse response (FIR) filter, 3380th order) and then notch filtered at 50 Hz (Hamming window FIR, 846th order) to remove power line noise. Artifact subspace reconstruction (ASR) was then

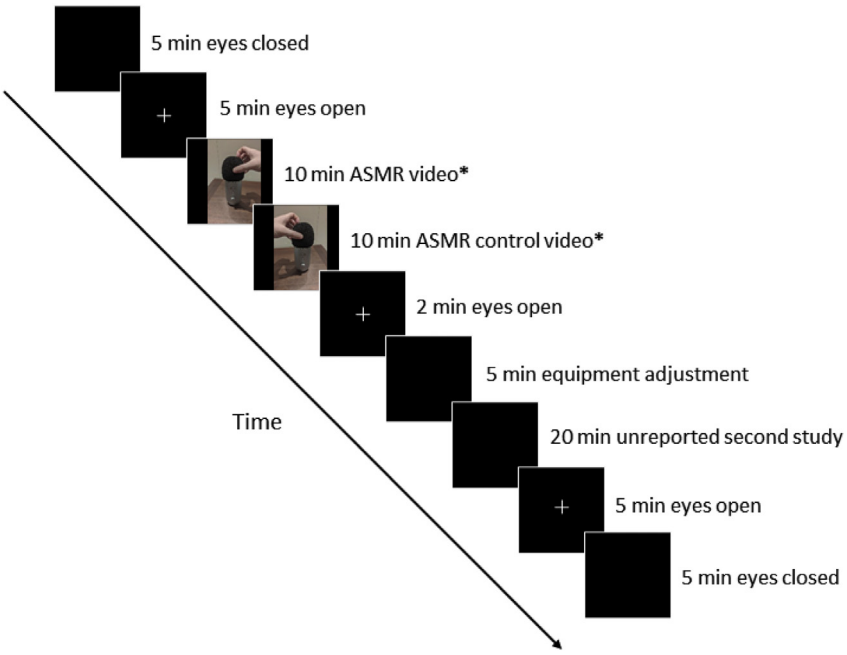

Fig. 1 – Schematic figure representing the timing of each recording block in the EEG experimental paradigm. First, each subject had 5 min of resting-state EEG and ECG recorded with eyes closed, and then 5 min with eyes open. Subsequently, two ASMR videos were watched whilst reporting what state was currently being experienced, with a 2-min presentation of a fixation cross between them. Then, a 2-min fixation cross, followed by another unreported study, were presented. Finally resting state was recorded again. *The order of the ASMR experimental video and ASMR control video was counterbalanced across the participant group. Thus, the control ASMR video originated from the same ASMR experimental video, except the temporal continuity was randomly shuffled every 5 s.

used to detect noisy channels and then spherically interpolate them before running independent components analysis (ASR from the clean_rawdata EEGLAB plugin [Kothe & Makeig, 2013; Mullen et al., 2015],). Principal component analysis-weight adjusted ICA (runica) was then used per participant to remove VEOG, HEOG, and heartbeat-related components (mean 2.54 components removed, SEM .16).

After, the data were segmented into non-overlapping epochs of 2 s, labelled to reflect the subjective states indicated by the participant (Baseline; Relaxed; WeakASMR; StrongASMR). The first epoch of each state was excluded to avoid interference activity related to the button press. Next, an artefact rejection threshold of ± 80 μV was applied, and any epoch exceeding this threshold were rejected (this exclusion criteria was established before analysis; mean 17% epochs removed, SEM 2.45, where the mean total remaining epochs were 437, SEM 13.56). Finally, epochs containing visible artifacts such as muscle activity and eye-movements/saccades were rejected using visual inspection.

ECG data, calculated as the difference between the two ECG electrodes, were used to extract metrics of heart-rate (HR) and heart rate variability (HRV). Prior work has shown that ASMR reduces HR (Poerio et al., 2018). In addition, increases in resting HRV (vagally-mediated) have been linked to emotional processing by the prefrontal cortex (Mccraty & Shaffer, 2015). Since ASMR-responders report a calming effect from ASMR-inducing stimuli, we predict that HRV scores would be higher during and after experiencing ASMR. Epochs below a threshold of 10 s were excluded. Inter beat intervals and HRV were calculated using the HRVTool MATLAB toolbox and its rrHRV method (Vollmer, 2015, 2019). Specifically, the HRV metrics extracted from the ECG signal were the root mean square of successive RR interval differences (RMSSD), high-frequency HRV (HF-HRV; Fast-Fourier-Transformation, bandwidth .15–.4 Hz), and low-frequency HRV (LF-HRV; Fast-Fourier-Transformation, bandwidth .04–.15 Hz, Camm et al., 1996).

2.5. *Spectral analysis*

The characteristic power spectral density was taken for each event state (Baseline, Relaxed, WeakASMR, StrongASMR) (in mV^2/Hz) from the EEG data using multitaper discrete prolate spheroidal sequences (DPSS). First, power was calculated from 1 to 80 Hz in steps of 1 Hz with spectral smoothing of 2 Hz—achieving high-frequency resolution (Oostenveld et al., 2011). Then, the mean power was calculated in each state for each participant by averaging of the segments of a given state, and then normalised by the total power across 1–80 Hz.

2.6. *ASMR decay effect*

Since an ASMR decay effect of unknown duration was hypothesised, the 'Baseline' and 'Relaxed' self-report states were subdivided by their relation in time to the ASMR states (WeakASMR, StrongASMR). Once either WeakASMR or StrongASMR was reported, any subsequent states of Baseline or Relaxed were labelled as PostASMR by adding the prefix

'Post' to the event labels, respectively (PostBaseline, PostRelaxed). Similarly, Baseline or Relaxed states reported before ASMR being achieved by the participant were labelled as PreASMR by adding the prefix 'Pre' (PreBaseline, PreRelaxed). These state-specific data epochs were collated if a participant left and re-entered a state multiple times throughout the video.

2.7. EEG source reconstruction

Collecting individual brain images of the participants was not feasible, and thus we relied on an average template on MNI space. A single template-based forward model was constructed based on the default average MNI brain coordinates. The head model consisted of a three-layer boundary element (BEM) model, generated using the whole-head tissue probability map provided with the NY Head (Huang et al., 2016). The three layers were defined as the inner skull (interface between the brain cavity and the skull), the outer skull (interface between the skull and the soft tissue of the scalp), and the scalp (outer layer of the skin). We used a homogeneous regular grid of dipoles defined in MNI space and with a separation of 10 mm, as source model. The final source model consisted of 2459 sources located inside the brain cavity (inner skull surface), and each dipole was labelled according to the Automated Anatomical Labeling (AAL) atlas (Tzourio-Mazoyer et al., 2002). The electrode positions were extracted from the standard definition for the 10-05 system provided by Robert Oostenveld in FieldTrip (Oostenveld et al., 2011). Finally, the forward model was built using a symmetric BEM approach as implemented in OpenMEEG (Gramfort et al., 2010). As the inverse method, we used a spatial filter based on dynamic imaging of coherent sources (DICS) beamformer (Gross et al., 2001). The spatial filters were calculated separately for each band using the frequency ranges obtained from sensor-space cluster-based permutation tests, using the average cross-spectral density matrix for all the frequency steps in the band, and using a regularisation factor of 5% of the average sensor power. Subsequently, each spatial filter was used to reconstruct each frequency step in the band for each source position. The input to the spatial filter is the Fourier transform of the time series of each channel for the frequencies in the band of interest, and the output is the Fourier transform of the time series of each source position. Subsequently, we obtained the per-frequency power by the averaged (for epochs) periodogram and normalized it by the broadband power (1–80 Hz). Finally, we calculated the relative power in the band of interest for each source position by adding all the frequency steps belonging to this band.

2.8. Statistical analysis

Due to the unreliable nature of ASMR induction and thus the variable number of epochs for each participant in each state, WeakASMR and StrongASMR were combined into one state (henceforth termed ASMR, unless otherwise specified).

2.8.1. Temporal scrambling (control videos)

Paired *t*-tests were used to compare the effect of temporal scrambling on ASMR stimuli for use as an effective control (whilst still keeping low-level features equivalent). Specifically, the duration of each state was contrasted between ASMR and control videos.

2.8.2. Sensor-level

FieldTrip power data structures were used for statistical analysis at the sensor level, using two-tailed cluster-based permutation tests (CBPTs) with a threshold correction to control for the multiple comparisons problem at level .05 (5000 iterations; Maris & Oostenveld, 2007; Oostenveld et al., 2011). Each contrast was performed across all 64 electrodes at each of the following frequency bands: delta (1–4 Hz), theta (4–8 Hz), alpha (8–13 Hz), beta (13–30 Hz), gamma (30–80 Hz). For each statistical contrast plot (Figs. 2–3), the above-normalised power of each frequency band was calculated as a percentage change from the contrast condition. Cohen's d effect sizes were subsequently calculated using the mean of all electrodes in the significant cluster using the FieldTrip toolbox.

The statistical contrasts used for both sensor and source space were divided into two categories. Firstly, the identification of the hypothesised steps for ASMR induction: i) Stage 1 was calculated from PreRelaxed vs PreBaseline, ii) Stage 2 was calculated from ASMR vs PreRelaxed, and iii) a summary contrast of ASMR vs PreBaseline was calculated in the event of a non-linear ASMR induction process. StrongASMR was also contrasted against WeakASMR to test the spectral differences between these distinct ASMR intensities.

The second category was the identification of potential decay effects of ASMR.These decay effects were defined as persisting oscillatory changes in the absence of self-reported ASMR (PreRelaxed *vs* PostRelaxed). For example, the video stimuli and self-report states between PreRelaxed and PostRelaxed are equivalent (and likewise with PreBaseline *vs* PostBaseline). Therefore, we define any difference between these two states as attributable to a decay effect of ASMR.

Approximate time windows for the decay effect of ASMR were estimated by comparing the Relaxed and Baseline contrasts. PostRelaxed vs PreRelaxed was estimated to be an immediate decay effect. PostBaseline vs PreBaseline was estimated to be on the scale of seconds to minutes. Finally, the eyes-open resting states recorded at the start and the end of the experiment were used to estimate a time window between 5 and 30 min. Assuming a participant experienced ASMR at the end of the second (unreported) EEG study, we estimate that 5 min would be the minimum possible duration. Similarly, assuming a participant only experienced ASMR within the first 5 min, an estimated maximum of 45 min is possible.

2.8.3. Source-level

Results from the sensor-space analysis were then used to inform the comparisons in the source-space. Specifically, the frequency sub-bands and the direction of the differences (tail) were applied in this exploratory source analysis. Finally, we implemented the false discovery rate (FDR) using an adaptive linear step-up procedure with a threshold set to a level of $q = .05$ (Benjamini et al., 2006, code freely available at https://uk.mathworks.com/matlabcentral/fileexchange/27423-two-stage-benjamini-krieger-yekutieli-fdr-procedure). This control provided an adapted threshold *P*-value (termed P_{FDR}).

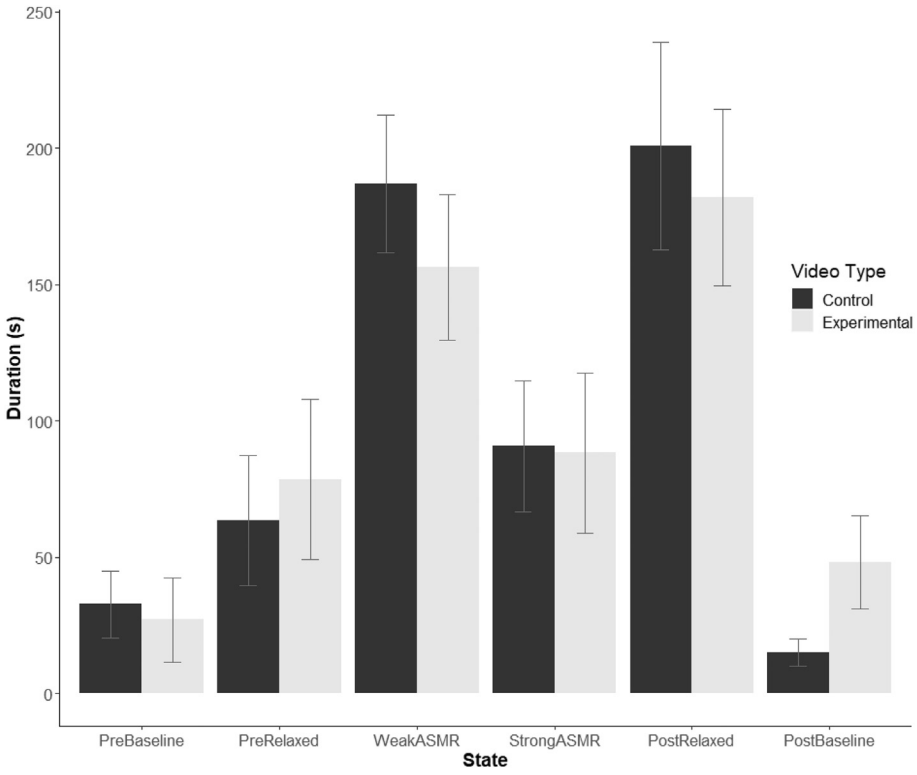

Fig. 2 – Experimentally-induced changes to the duration of self-reported states throughout watching each ASMR video. Experimental videos were personalised 10 min ASMR videos. Control videos contained the same content, except that the content was temporally shuffled every 5 s within the 10 min. Error bars represent SEM. *$p < .05$.

Statistical tests were performed using one-tailed permutation tests with a cluster-based threshold correction to control for the multiple comparisons problem at level .05 (10,000 iterations; Maris & Oostenveld, 2007; Oostenveld et al., 2011). Effect sizes were subsequently calculated from the mean of all voxels in the significant cluster. Cortical regions are labelled following the AAL atlas and are stated in the results given below if more than 50% of the region was significant. To further refine and improve the clarity of effects in each contrast, where possible, the cluster alpha level was reduced from .05 by increments of .01, then .001 and so on until the number of significant regions was lower than 10. These normalised powers were then calculated as a percentage change from the contrast condition in Figs. 4–5.

When an effect was to be expected (for example, a specific band of interest found in related literature) but did not appear in sensor space, we also evaluated it using a two-tailed approach (as we did not know the direction of the effect), and the results were subsequently corrected for multiple comparisons. These results are labelled in the figure as "not matching sensor-space hypothesis" and marked with the sign ◊(Table 1).

2.8.4. *Heart-rate variability*

For HR, we performed a one-tailed *t*-test of ASMR compared to PreRelaxed and PreBaseline, where a reduction in HR in the ASMR group was expected (Poerio et al., 2018). Mean HRV values in each state were contrasted using paired *t*-tests. RMSSD scores were tested by contrasting ASMR vs PreRelaxed, ASMR vs PreBaseline and PreRelaxed vs PreBaseline. In addition, following the same format for the decay contrasts, the Relaxed, Baseline and resting-state contrasts were also performed (Post *vs* PreASMR). All HRV tests were FDR-controlled using the adaptive linear step-up procedure ($q = .05$ (Benjamini et al., 2006);).

3. Results

3.1. *The effect of temporal scrambling on ASMR*

Paired *t*-tests compared all six states between experimental and control videos, where temporal scrambling was the applied intervention. The PostBaseline contrast was the only contrast that showed a significant difference due to scrambling ($t(24) = -2.10$, $P = .046$, $d = -.42$, Fig. 2). The PreBaseline ($t(24) = .41$, $P = .69$), PreRelaxed ($t(24) = -.56$, $P = .58$), WeakASMR ($t(24) = 1.16$, $P = .26$), StrongASMR ($t(24) = .18$, $P = .86$) and PostRelaxed ($t(24) = .50$, $P = .62$) contrasts revealed no significant differences.

Since there were no significant differences shown for ASMR induction, state-specific epochs of both video types were collapsed together for the TF analysis below. Whilst there was a significant difference for the PostBaseline contrast, the effect size was small, and thus the decision was made to incorporate to boost the sample size.

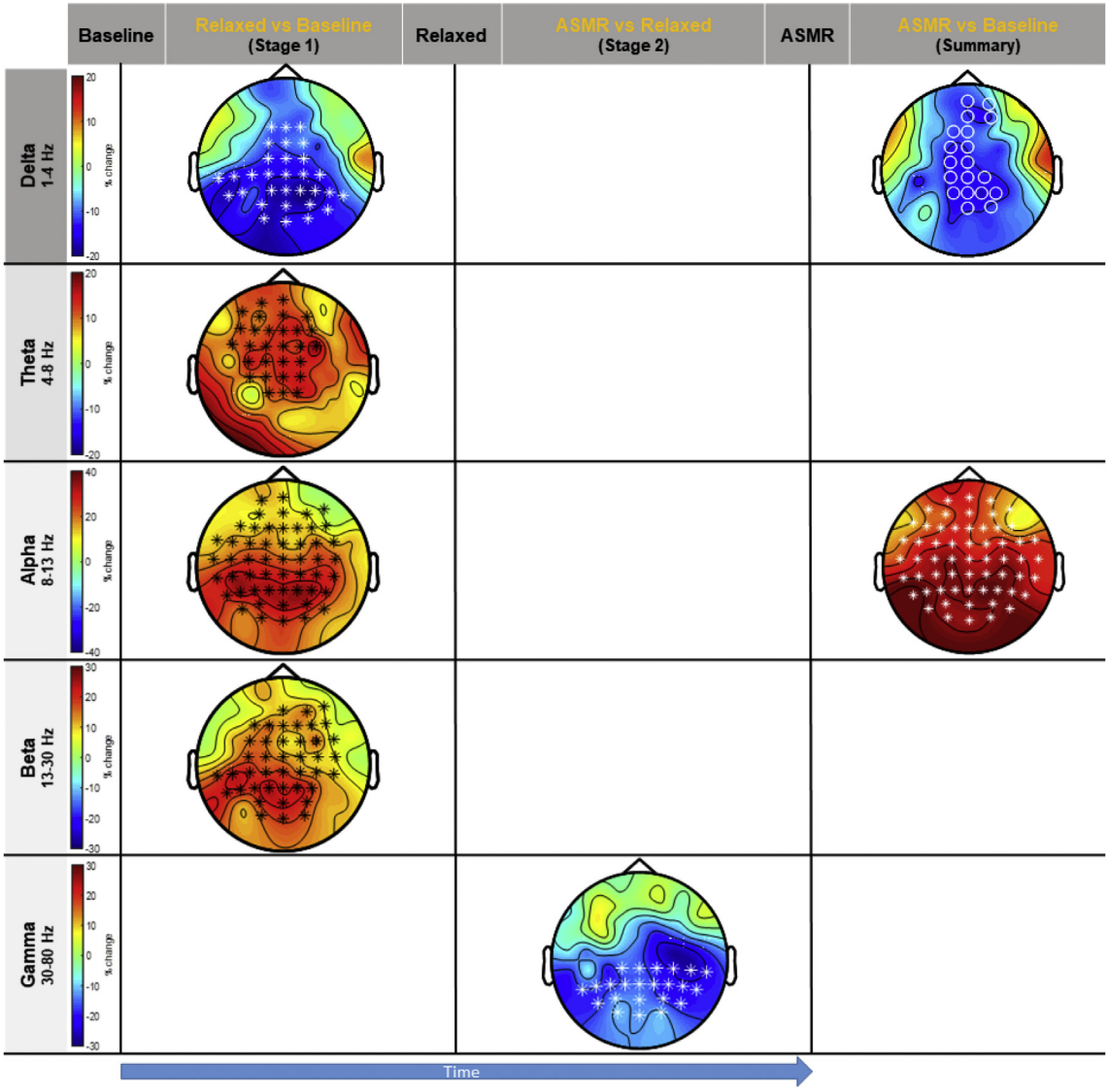

Fig. 3 – Sensor-space ASMR stage contrast. Cluster-based random permutation tests were performed in the sensor-space comparing PreRelaxed vs PreBaseline; ASMR vs PreRelaxed; and ASMR vs PreBaseline (showed in columns) under the classical frequency bands (rows). Topographical plots are shown representing the proportional change from PreBaseline, PreRelaxed and PreBaseline, respectively. For Stage 1, PreRelaxed showed a significant decrease in delta at central and parietal sites ($p = .0036$); a significant increase in theta at central and frontocentral sites ($P = .0066$); an increase in alpha globally ($P = .0016$); and increase in beta power centrally ($p = .0108$). For Stage 2, ASMR showed a significant decrease in gamma power at posterior sites ($P = .0124$). For the summary contrast, ASMR decreased delta power centrally ($p = .0176$) and increased alpha globally ($P = .0006$). The progression in time has been represented by a change from PreBaseline to PreRelaxed to ASMR. The ASMR vs Baseline column represents the summary change. $^{\circ}p < .05$, $^{*}p < .01$. Colour of the topographical symbols have been modified where appropriate (from black to white) to improve contrast.

3.2. *Heart-rate variability*

No effects survived correction and thus have been reported in the Supplementary.

3.3. *TF responses*

3.3.1. *Oscillatory correlates of ASMR (sensor)*

ASMR significantly modulated participants' oscillatory activity compared with a PreRelaxed and PreBaseline state (see Fig. 3). When comparing the ASMR state relative to the PreRelaxed state ($n = 23$), we discovered a significant decrease in high gamma, primarily across posterior electrodes (50–72 Hz, one negative cluster, $P = .0124$, $d = .55$). Moreover, when comparing the difference between ASMR and PreBaseline states ($n = 17$), statistical testing revealed significantly lower delta power at central and frontocentral sites (1–2 Hz, one negative cluster, $P = .0176$, $d = .63$). In addition, a significant increase in alpha power was discovered in ASMR, increasing most strongly at posterior electrodes (9–13 Hz,

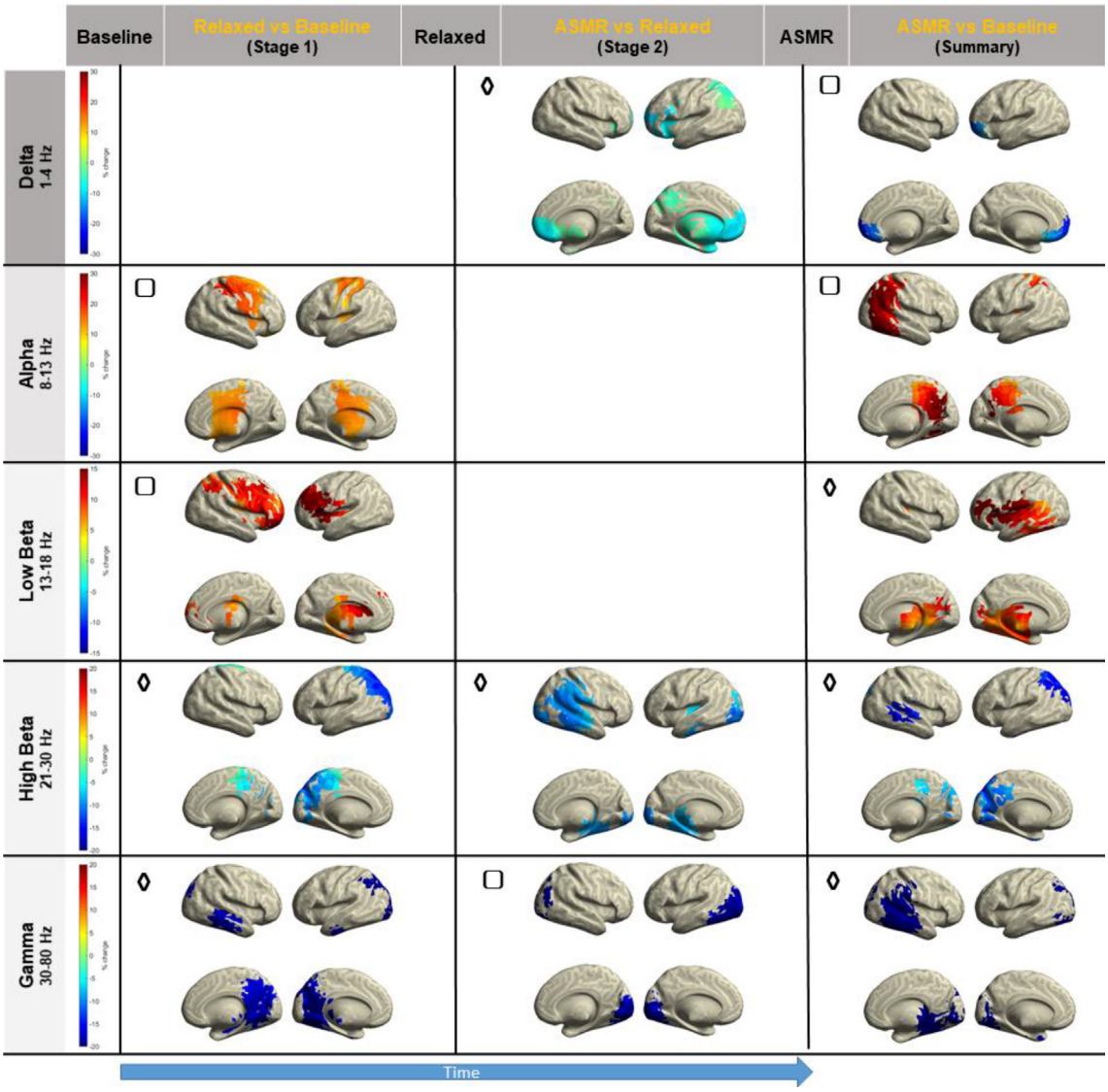

Fig. 4 – Source-space ASMR stage contrast. Cluster-based random permutation tests were performed in the source-space comparing PreRelaxed vs PreBaseline; ASMR vs PreRelaxed; and ASMR vs PreBaseline under sub-bands of the classical frequency bands based on the sensor-space analysis (see Fig. 3). Surface plots are shown representing the proportional change from PreBaseline, PreRelaxed and PreBaseline respectively. The progression in time has been represented by a change from PreBaseline to PreRelaxed to ASMR. The ASMR vs Baseline column represents the summary change. For Stage 1, PreRelaxed showed a significant increase in alpha in parietal, frontal and temporal regions ($P_{FDR} < .05$), increase in low beta in frontal and temporal regions ($P_{FDR} < .05$), decrease in high beta in occipital and parietal regions ($P_{FDR} < .05$), and a decrease in gamma in occipital regions ($P_{FDR} < .05$). For Stage 2, ASMR showed a significant decrease in the delta in frontal regions ($P_{FDR} < .05$), a decrease in high beta in temporal regions ($P_{FDR} < .05$) and a decrease in gamma in occipital regions ($P_{FDR} < .05$). For the summary contrast, ASMR showed a significant decrease in the delta in frontal regions ($P_{FDR} < .05$), increase in alpha in parietal regions ($P_{FDR} < .05$), increase in low beta in occipital and temporal regions ($P_{FDR} < .05$), decrease in high beta in occipital and parietal regions ($P_{FDR} < .05$), and a decrease in gamma in temporal regions ($P_{FDR} < .05$). ▫ indicates a matching sensor-space hypothesis; ◊ indicates no matching sensor-space hypothesis.

one positive cluster, $P = .0006$, $d = .73$). Lastly, more beta power was present in ASMR relative to PreBaseline (13–14 Hz, trend-level positive cluster, $P = .0284$, $d = .69$).

Significant differences in the spectral profile of the PreRelaxed state were discovered when compared with the PreBaseline state ($n = 19$, see Fig. 3). PreRelaxed delta power decreased at central and bilateral parietal electrodes (1–2 Hz, one negative cluster, $P = .0036$, $d = .65$, Fig. 3). Also, an increase in theta power was found in the PreRelaxed state, with theta power increasing across central and frontocentral electrodes (4–6 Hz, one positive cluster, $P = .0066$, $d = .60$, Fig. 3). A higher change in alpha power was also discovered in the PreRelaxed relative to the PreBaseline comparison, in one positive cluster over central parietal regions and frontal central regions (10–13 Hz, $p = .0016$, $d = .62$). Lastly, an increase in beta power was shown in PreRelaxed across central and right central

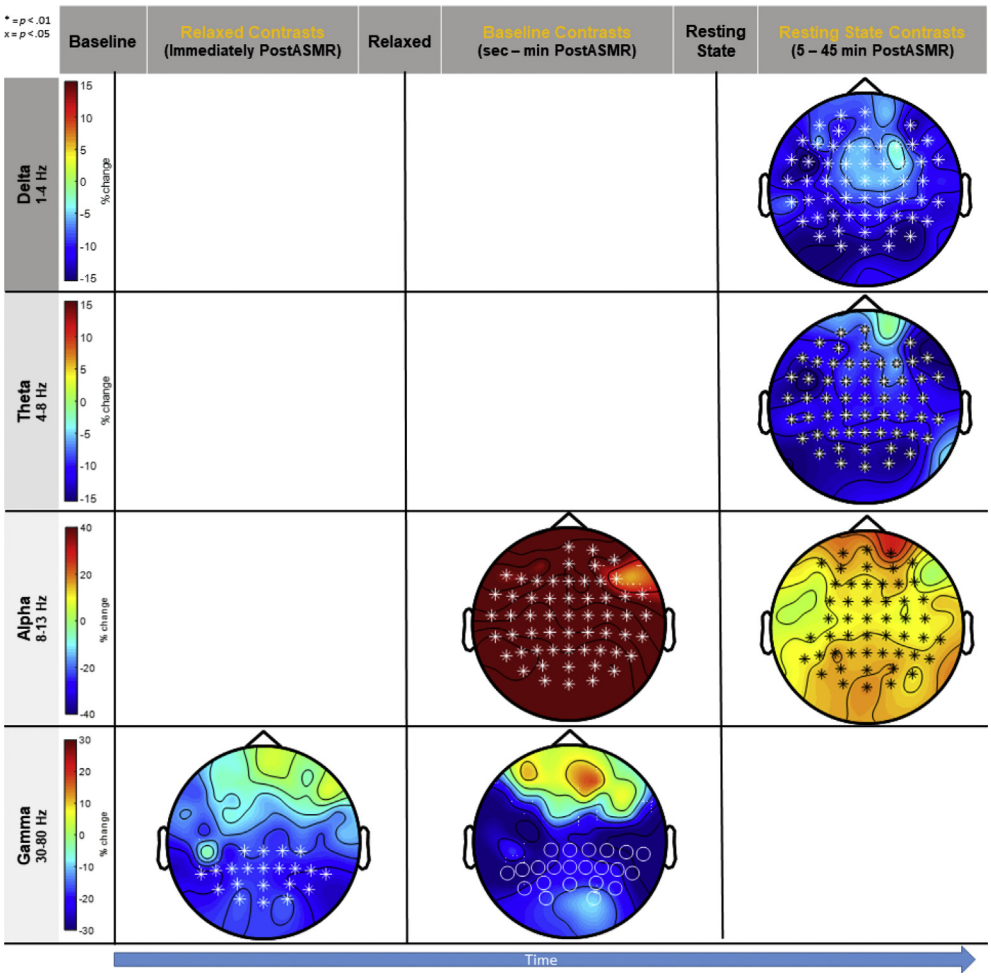

Fig. 5 – Sensor-space ASMR decay contrast. Cluster-based random permutation tests were performed in the sensor-space comparing PostRelaxed vs PreRelaxed (representing Relaxed state data that immediately follow the end of a period of ASMR tingles); PostBaseline vs PreBaseline (representing Baseline data that typically occurred on a timescale between seconds and minutes after a period of ASMR tingles); and PostASMR Resting-state vs PreASMR resting state under the classical frequency bands. Topographical plots are shown representing the proportional change from PreRelaxed, PreBaseline and PreASMR resting-state, respectively. For the Relaxed contrasts, PostRelaxed showed a significant negative decrease in gamma power posteriorly ($P = .0092$). For the Baseline contrasts, PostBaseline showed a significant increase in alpha power globally ($P = .0008$); and a decrease in gamma power posteriorly ($P = .0156$). For the resting state contrasts, the PostASMR resting-state showed a significant decrease in delta power globally ($P = .0004$), a decrease in theta power globally ($P = .0006$), and an increase in alpha power globally ($P = .0008$). The progression in time has been represented by a change from PostRelaxed to PostBaseline to PostASMR resting state. The scale of the timeframe or the theoretical ranges is shown under the title of each column. °$p < .05$, *$P < .01$. Colour of the topographical symbols have been modified where appropriate (from black to white) to improve contrast.

electrodes and central posterior and left parietal electrodes (13–18 Hz, one positive cluster, $P = .0108$, $d = .63$, see Fig. 3).

3.3.2. *Oscillatory correlates of ASMR (source)*

Sensor space tests revealed two prominent beta ranges used below: low beta (13–18 Hz) and high beta (21–30 Hz).

We discovered five source space effects that survived corrections when comparing the ASMR state to the Pre-Baseline state ($n = 17$). Firstly, a decrease in delta most prominent in frontal regions was revealed (1–2 Hz, one significant negative cluster, cluster alpha = .003, $P_{FDR} < .05$, $d = .78$). The associated regions were bilateral gyri recti (REC), left inferior frontal gyrus (orbital, ORBinf), left middle frontal gyrus (orbital, ORBmid), bilateral superior frontal gyri (medial orbital, ORBsupmed), and bilateral superior frontal gyri (orbital, ORBsup). Secondly, an increase in alpha most prominent in the cingulate and parietal gyri was revealed (9–13 Hz, one significant positive cluster, cluster alpha = .0005, $P_{FDR} < .05$, $d = 1.00$). More specifically, the following regions were shown to be significantly implicated (>50% regional association with the cluster): bilateral posterior cingulate gyri (PCG), right angular gyrus (ANG), right inferior parietal gyrus (IPG), and right precuneus (PCUN, see Fig. 4). One other significant effect in the ASMR state was an

Table 1 – Identified regions of interest included in the AAL-atlas.

Regions	Abbreviations	Regions	Abbreviations
Rolandic operculum	ROL	Inferior temporal gyrus	ITG
Cuneus	CUN	Middle frontal gyrus, orbital part	ORBmid
Lingual gyrus	LING	Inferior frontal gyrus, orbital part	ORBinf
Superior occipital gyrus	SOG	Inferior frontal gyrus, triangular part	ORBtriang
Middle occipital lobe	MOL	Inferior frontal gyrus, opercular	ORBoperc
Inferior occipital lobe	IOL	Superior frontal gyrus (medial orbital)	ORBsupmed
Fusiform gyrus	FFG	Superior frontal gyrus (orbital)	ORBsup
Superior parietal gyrus	SPG	Gyrus rectus	REC
Inferior parietal gyrus	IPG	Anterior cingulate and paracingulate gyri	ACG
Supramarginal gyrus	SMG	Posterior cingulate gyrus	PCG
Angular gyrus	ANG	Precentral gyrus	PreCG
Precuneus	PCUN	Calcarine fissure and surrounding cortex	CALC
Paracentral lobule	PCL	Postcentral gyrus	PoCG
Superior temporal gyrus	STG	Heschl gyrus	HES
Middle temporal gyrus	MTG	Insula	INS

increase in low beta, most prominently in occipital and temporal regions (13–18 Hz, one significant positive cluster, cluster alpha = .0004, $P_{FDR} < .05$, $d = 1.06$). The associated regions were left fusiform gyrus (FFG), left Heschl's gyrus (HES), left inferior temporal gyrus (ITG), left lingual gyrus (LING), left middle temporal gyrus (MTG), left rolandic operculum (ROL) and left superior temporal gyrus (STG, see Fig. 4). A fourth effect was a decrease in high beta in ASMR, most prominent in occipital and parietal regions (21–30 Hz, one significant negative cluster, cluster alpha = .0001, $P_{FDR} < .05$, $d = 1.20$). The associated regions were left calcarine fissure and surrounding cortex (CALC), PCG-L, left cuneus (CUN), left superior occipital gyrus (SOG) and left superior parietal gyrus (SPG). The final result from the ASMR to PreBaseline state comparison was a decrease in higher gamma, most prominent in temporal regions (50–72 Hz, one significant negative cluster, cluster alpha = .00001, $P_{FDR} < .05$, $d = 1.06$). The associated regions were FFG-R, ITG-R, MTG-R, STG-R and the supramarginal gyrus (SMG).

Three significant differences in the ASMR state's spectral profile were discovered compared with the PreRelaxed state ($n = 23$, see Fig. 4). Firstly, a decrease in delta power most prominent in frontal regions was seen (1–2 Hz, one significant negative cluster, cluster alpha = .02, $P_{FDR} < .05$, $d = .51$). The regions associated were ANG-L, bilateral anterior cingulate gyri (ACG), REC-LR, ORBinf-L, ORBmid-L, ORBsupmed-LR, ORBsup-LR, SPG-L and left temporal pole (middle temporal gyrus, MTG). Secondly, a decrease in high beta most prominent in temporal regions (21–30 Hz, one significant negative cluster, cluster alpha = .002, $P_{FDR} < .05$, $d = .72$). Specifically, the regions associated were MTG-R, STG-R and SMG-R. Finally, a decrease in gamma most prominent in occipital regions was revealed (50–72 Hz, one significant negative cluster, cluster alpha = .00005, $P_{FDR} < .05$, $d = 1.21$). The regions associated were CALC-L, bilateral inferior occipital lobe (IOL), left middle occipital lobe (MOL) and the LING-LR.

We discovered four effects that survived corrections when comparing the PreRelaxed state to the PreBaseline state ($n = 19$). An increase in alpha most prominent in parietal, frontal and temporal regions (10–13 Hz, one significant positive cluster, cluster alpha = .005, $P_{FDR} < .05$, $d = .68$). The regions associated were bilateral middle cingulate gyri (MCG), left paracentral lobule (PCL), bilateral postcentral gyri (PoCG), bilateral rolandic operculum (ROL), ORBmid-R, and right precentral gyrus (PreCG, see Fig. 4). Secondly, a significant increase in low beta most prominent in frontal and temporal regions was revealed (13–18 Hz, one significant positive cluster, cluster alpha = .005, $P_{FDR} < .05$, $d = .71$). The associated regions were HES-L, bilateral inferior frontal gyri (opercular, ORBoperc), bilateral inferior frontal gyri (triangular, ORBtriang), left insula (INS), IPG-R, ORBmid-R, ROL-R, and ORBsup-R. Thirdly, a significant decrease in high beta, most prominent in occipital and parietal regions, was revealed (21–30 Hz, one significant negative cluster, cluster alpha = .002, $P_{FDR} < .05$, $d = .82$). The regions associated were ANG-L, CUN-L, IPG-L, MOL-L, PCUN-L, SOG-L, SPG-L, and PCL-R. Finally, a significant decrease in gamma was revealed most prominently in occipital regions (50–72 Hz, one significant negative cluster, cluster alpha = .00005, $P_{FDR} < .05$, $d = .98$). Specifically, the association regions were CUN-LR, LING-LR, SOG-L, and CALC-R (see Fig. 4).

3.3.3. *Decay effects of ASMR (sensor)*

A significantly lower high gamma power was discovered when testing the decay effects of ASMR using the PostRelaxed and PreRelaxed states ($n = 21$). This cluster was most prominent across posterior electrodes (52–80 Hz, one significant negative cluster, $P = .0092$, $d = .56$, see Fig. 5).

When testing the difference between PostBaseline and PreBaseline states ($n = 10$) we found significantly higher power in PostBaseline alpha, globally (10–13 Hz, one significant positive cluster, $P = .0008$, $d = .80$, see Fig. 5). Also, we observed a significant decrease in gamma power at posterior electrodes (59–76 Hz, one significant negative cluster, $P = .0156$, $d = .85$) and higher beta power at frontal and central electrodes (13–14 Hz, one trend-level positive cluster, $P = .0274$, $d = .86$).

PostASMR eyes-open resting state was also found to exhibit significantly lower delta and theta power, in all electrodes, when compared to PreASMR eyes-open resting states ($n = 25$; 1–4 Hz, one significant negative cluster, $P = .0004$, $d = .75$; 4–5 Hz, one significant negative cluster, $P = .0006$, $d = .71$, see Fig. 5). Finally, PostASMR eyes-open resting state was revealed

to be characterised by higher alpha power (10–13 Hz, one significant positive alpha cluster, $P = .0008$, $d = .61$).

3.3.4. *Decay effects of ASMR (source)*

When comparing PostRelaxed with PreRelaxed ($n = 21$), two effects survived corrections. The first effect revealed was a decrease in high beta, most prominent at occipital and temporal regions (21–30 Hz, one significant negative cluster, cluster alpha = .001, $P_{FDR} < .05$, $d = .80$). Specifically, the association regions were FFG-R, IOL-R, ITG-R, LING-R, and MOL-R. The second effect was a significant decrease in gamma primarily in occipital regions (52–80 Hz, one significant negative cluster, cluster alpha = .00007, $P_{FDR} < .05$, $d = .80$). The associated regions were CALC-L, IOL-L, LING-LR, and MOL-L (see Fig. 6).

Testing the difference between PostBaseline and PreBaseline ($n = 10$), three effects were revealed. The first effect was a significant increase in alpha most prominent at parietal regions (10–13 Hz, one significant positive cluster, cluster alpha = .001, $P_{FDR} < .05$, $d = 1.27$). The associated regions were MCG-L, ANG-R, IPG-R, PCUN-R, and SPG-R (see Fig. 6). Secondly, a significant decrease in high beta was revealed most prominently at occipital and parietal regions (21–30 Hz, one significant negative cluster, cluster alpha = .0003, $P_{FDR} < .05$, $d = 1.69$). The associated regions were ANG-L, CALC-L, PCG-LR, CUN-L, MOL-L, and SOG-L. Finally, a significant decrease in gamma was revealed most prominently at occipital and temporal regions (59–76 Hz, one significant negative cluster, cluster alpha = .00003, $P_{FDR} < .05$, $d = 2.16$). The associated regions were PCG-LR, LING-L, FFG-R (see Fig. 6).

PostASMR eyes-open resting state was also compared with PreASMR eyes-open resting state ($n = 25$), where four significant differences were revealed. Firstly, delta power was significantly lower in PostASMR, most prominently in occipital and parietal regions (1–4 Hz, one significant negative cluster, cluster alpha = .00002, $P_{FDR} < .05$, $d = .82$, see Fig. 6). Specifically, the regions associated were ANG-L, MOL-L, and PCUN-LR. Secondly, a significant decrease in theta power was revealed, most prominently in occipital regions (4–5 Hz, one significant negative cluster, cluster alpha = .0001, $P_{FDR} < .05$, $d = .81$). The regions associated were CALC-L, PCG-L, CUN-LR, MOL-L, PCUN-L, and SOG-LR. The third effect revealed was a significant increase in alpha most prominently over parietal regions (8–12 Hz, one significant positive cluster, cluster alpha = .001, $P_{FDR} < .05$, $d = .69$, see Fig. 6). The regions associated were PCUN-L, SPG-LR, ANG-R, IPG-R, and PCL-R. Finally, a significant increase in low beta power most prominently over frontoparietal regions was revealed (13–18 Hz, one significant positive cluster, cluster alpha = .005, $P_{FDR} < .05$, $d = .69$). The associated regions were ANG-L, IPG-L, PoCG-L, SPG-L, and SMG-L.

4. Discussion

This study aimed to reveal the neural correlates of ASMR experiences by investigating large-scale brain oscillations. We further source localised the ASMR-induced oscillatory changes and their potential decay effects. First, we demonstrated that ASMR, compared to baseline, was associated with a robust change in five frequency bands over a multitude of brain regions. Specifically, we found decreases in delta power in prefrontal regions; increases in alpha power in parietal, frontal, and temporal regions; increases in low beta power in parietal and temporal regions, decreases in high beta power in parietal and occipital regions, and decreases in gamma power in occipital regions. Second, we observed a decay effect of ASMR in the absence of self-reported ASMR tingling sensations. Third, the temporal profile of the modulations by ASMR in high-frequency power later shifts to lower frequencies (1–8 Hz), except for enhanced alpha which persists for up to 45 min post self-reported ASMR. Finally, we showed that the temporal continuity of the ASMR-inducing video is not vital for ASMR induction.

Our findings support evidence provided by one prior study in which ASMR enhances alpha power during the experience (Fredborg et al., 2021). This positive effect was seen globally at the sensor level, with greater enhancement in occipital-parietal areas. According to the alpha inhibition-timing hypothesis, large alpha represents inhibitory processes that can be either attributed to relaxed mental inactivity (unspecific inhibition) or during active cognitive processes that require (process-specific) inhibition of distracting stimuli/less relevant brain regions (Klimesch et al., 2007). Moreover, it is hypothesised that when reference/baseline alpha power is small, the brain is primed for good perceptual performance. Thus, it is plausible that the alpha enhancement seen in the PreRelaxed vs PreBaseline and ASMR vs PreBaseline source contrasts represents a low reference alpha in the PreBaseline condition. Accordingly, we speculate this finding represents an initial high degree of multisensory processing whilst watching the ASMR stimuli. Subsequently, alpha power increases, thereby reflecting an enhanced state of relaxation (as indicated by the participant). There is no additional significant enhancement of alpha in the ASMR vs PreRelaxed source contrast, perhaps indicating no significantly enhanced relaxation, although the relative enhancement appears to be greater when comparing PreRelaxed and ASMR vs PreBaseline contrasts. Another interpretation (which is not mutually exclusive) of this enhanced alpha is that once this relaxed state has been achieved, stimuli from the external environment are suppressed in preference for internally-oriented attention (Cooper et al., 2006; Magosso et al., 2019; Matsuoka et al., 2021). In this way, alpha synchronisation has been associated previously with internal mental processes such as self-referential thought and social cognition (Knyazev et al., 2011). Curiously, sensorimotor areas are implicated in the PreRelaxed vs PreBaseline source contrast, whilst regions associated with the default mode network (DMN) are implicated in the ASMR vs PreBaseline contrast. Alternatively, instead of inhibiting the processing of external stimuli altogether, this alpha activity could suggest a selective inhibition of stimuli through the inhibition of task-irrelevant brain regions (Jensen & Mazaheri, 2010; Klimesch et al., 2007; Symons et al., 2016). For example, Worden et al. have shown enhanced alpha oscillations in visual regions ipsilateral to attentionally-cued visual stimuli (Worden et al., 2000). In the context of emotion perception, it has been suggested that alpha oscillations may facilitate the selection of emotionally salient social cues through this inhibitory role (Symons et al., 2016).

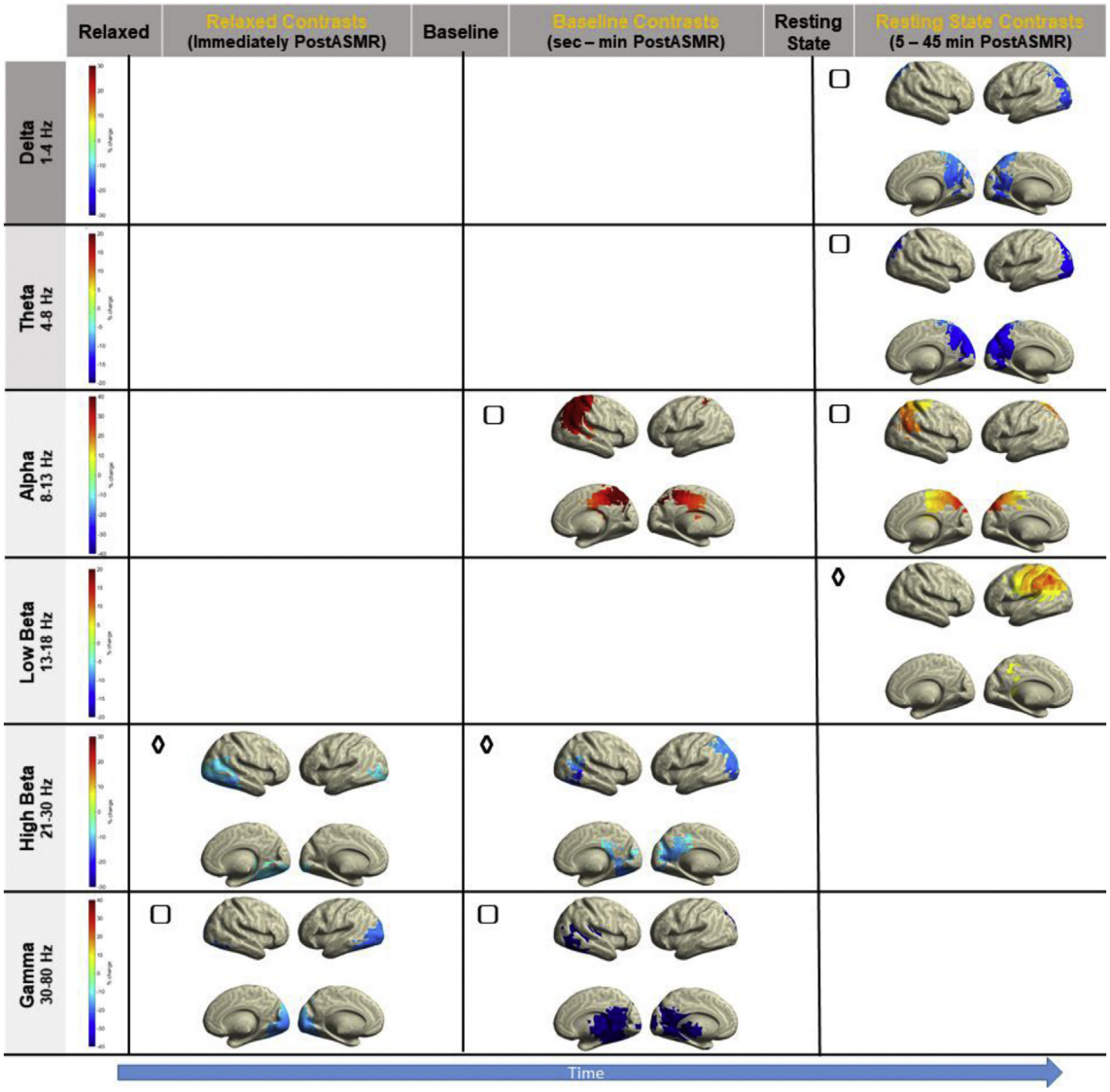

Fig. 6 – Source-space ASMR decay contrast. Cluster-based random permutation tests were performed in the source-space comparing PostRelaxed vs PreRelaxed; PostBaseline vs PreBaseline; and PostASMR Resting-state vs PreASMR resting state under sub-bands of the classical frequency bands based on the sensor-space analysis (see Fig. 5). Surface plots are shown representing the proportional change from PreRelaxed, PreBaseline and PreASMR resting-state, respectively. The progression in time has been represented by a change from PostRelaxed to PostBaseline to PostASMR resting state. The scale of the timeframe or the theoretical ranges is shown under the title of each column. For the Relaxed contrasts, PostRelaxed showed a significant decrease in high beta in occipital and temporal regions ($P_{FDR} < .05$) and a decrease in gamma in occipital regions ($P_{FDR} < .05$). For the Baseline contrasts, PostBaseline showed a significant increase in alpha power in parietal regions ($P_{FDR} < .05$), a decrease in high beta in occipital and parietal regions ($P_{FDR} < .05$), and a decrease in gamma in occipital and temporal regions ($P_{FDR} < .05$). For the resting state contrasts, PostASMR eyes-open showed a significant decrease in the delta in occipital and parietal regions ($P_{FDR} < .05$), decrease in theta power in occipital regions ($P_{FDR} < .05$), increase in alpha in parietal regions ($P_{FDR} < .05$), and an increase in low beta in frontoparietal regions ($P_{FDR} < .05$).□ indicates a matching sensor-space hypothesis; ◊ indicates no matching sensor-space hypothesis.

The Baseline and Resting-State decay source contrasts, but not the Relaxed contrasts, show an enhancement of alpha power in regions more similar to the ASMR vs PreBaseline source contrasts. This finding supports the notion that the enhanced alpha power is not restricted to an enhanced relaxed state, but could instead be related to ASMR-induced activity relating to DMN regions. We speculate this decay effect could then support the altered functional connectivity of DMN activity found in ASMR-Responders by prior fMRI work (Smith et al., 2017).

Considering this alpha enhancement finding, the gamma power reduction in areas related to sensory processing (e.g., facial/visual/auditory processing in STG, FFG, CALC, LING) could be of interest. Previous work on auditory attention has shown a reduction in gamma power when attention was inwardly oriented, in contrast to attending to auditory stimuli

(Villena-González et al., 2018). Therefore, this could reflect a change in internally-oriented thinking in contrast to attending the ASMR stimuli. This pattern of alpha enhancement and gamma decrease has also been suggested to be a top-down control for more internally driven attention in another study (Mu & Han, 2010). However, it should be noted that, in that study, the time-frequency analysis was limited to 40 Hz, whilst the gamma effects reported here range between 50 and 80 Hz. Typically, gamma–band activity is enhanced when processing multisensory stimuli, especially visual stimuli (Chandrasekaran & Ghazanfar, 2009; Chen et al., 2010). For example, a significant gamma enhancement in the FFG was previously shown during visual stimulus encoding (Tallon-Baudry et al., 2005). This gamma prediction is more aligned with the results of the Fredborg et al. study, where they found an enhancement in gamma for the audio trials only (Fredborg et al. 2021). Due to the individualised ASMR content, faces were not consistent enough to drive this enhancement. Conversely, it could be argued that the non-ASMR conditions (PreBaseline/PreRelaxed) involved greater visual processing, which then was inhibited during the ASMR experience in preference to internal processing.

A novel finding, distinct from previous research, was the modulation of beta power by ASMR. Beta modulation has been found in tasks involving sensorimotor processing (Cheyne et al., 2003; Senkowski, 2005), auditory processing (Eulitz & Obleser, 2007), action observation (Cheyne et al., 2003), emotional recognition (Chen et al., 2010), or even the predictive coding of audiovisual stimuli (e.g., see Arnal & Giraud, 2012). These processes are all particularly relevant for processing ASMR stimuli and the perception of the ASMR tingling sensations. For example, when assessing auditory processing, one study has found prolonged event-related desynchronisation of upper beta (15–30 Hz, strongest at 24Hz) in a task designed to extract phonological features from speech (Eulitz & Obleser, 2007). A similar phenomenon might be occurring in the present study. Our high beta decrease in power shown could also be explained by the extraction of acoustically complex features from whispered or softly spoken speech in ASMR stimuli. Whispered speech is a common property present in ASMR stimuli (Barratt et al., 2017; Kovacevich & Huron, 2019), and whispering is also known to impoverish the quality of communication in terms of spectral acoustic information (Frühholz et al., 2016). Considering this reasoning with the inhibitory effect of the alpha seen during ASMR, the enhanced alpha may represent the suppression of distractors irrelevant to this goal of vocal processing. If ASMR stimuli do indeed prime the individual to be more capable of filtering distractors, this could explain the reported use of ASMR as a study aid (Kovacevich & Huron, 2019). An alternative explanation for the modulation in low beta-band power is the proposed maintenance of the current sensorimotor or cognitive state (Engel & Fries, 2010). Whilst speculative, it is possible that the beta band activity relates to the maintenance and monitoring of the induced state (Spitzer & Haegens, 2017).

Another novel finding was the decrease in delta power seen in both sensor and source space contrasts. Medial prefrontal regions are implicated, supporting prior neuroimaging findings (Fredborg et al., 2021; Smith et al., 2019b). It has been hypothesised that delta activity could be correlated with anticipation of a reward (e.g., see Knyazev, 2007). This could explain the decreases in delta power seen in the ASMR vs PreRelaxed and PreBaseline contrasts, where reference states have higher (anticipatory) delta powers. Alternatively, a decrease in reward-related delta power has been seen through the administration of legal psychoactive drugs such as caffeine (Hammond, 2003), tobacco (Knott et al., 2008), and alcohol (Sanz-Martin et al., 2011). Thus, the decrease in frontal delta here may represent reward-related processing. Moreover, it has been suggested that relative delta and alpha oscillatory powers are more strongly negatively correlated in adults but less so in childhood (Knyazev, 2007). It has also been proposed that the relative strength of inhibitory control increases during childhood (see Clark, 1996), where there is a concomitant shift of relatively low-frequency dominance (e.g., delta) to relative alpha dominance throughout development (Knyazev, 2007). We speculate this developmental enhancement in inhibitory control could be related to the onset of ASMR capability (or at least the self-reported recollection of onset), which is thought to be between late childhood (mean age of 8; Barratt & Davis, 2015) and preadolescence (mean age of 15; Poerio et al., 2018) for many ASMR-Responders.

To our knowledge, this is the first study to provide neurophysiological evidence of the persistent decay effects of ASMR. Our results show that in periods reported as identical by the participant (e.g., PostRelaxed vs PreRelaxed) and under comparable experimental conditions (e.g., same ASMR video), there are electrophysiological differences that can be seen up to 45 min. Notably, the enhanced alpha effect persists even after the ASMR experience has been reported to have ended. Therefore, there is electrophysiological evidence for prolonged ASMR-induced relaxation, which corroborates self-reported data. This finding supports the idea for ASMR to be used therapeutically. However, further investigation is required to determine how long these effects last and if there are adverse side effects to this end. Moreover, when comparing resting-state contrasts, a general trend of low frequency decreases in power with concomitant higher frequency enhancements can be seen. One fMRI-EEG resting-state study has provided evidence that this pattern of activation and deactivation represents cognitive functions such as self-reflection, working memory and language (Jann et al., 2010). Therefore, this ASMR-modulated resting state may reflect a greater degree of self-reflection.

The novel control design in this study has been shown not to elicit significant differences in ASMR state duration for ASMR-Responders. We hypothesised that by disrupting the temporal continuity of the ASMR videos, higher–order properties of the stimuli (like narrative) would be disrupted whilst maintaining lower–level properties (like lighting) across the video as a whole. Therefore, the core properties of the auditory and visual stimuli may be inherently sufficient for ASMR induction. Alternatively, individual differences within this result are likely being averaged out. Participants verbally reported either an enhancement of ASMR intensity (perhaps due to expectancy effects of their individualised videos) or a disruption of ASMR induction due to temporal scrambling. Therefore, these individual differences might portray different outcomes for different ASMR subtypes. For example, an ASMR-Responder who prefers repetitive sounds like tapping for ASMR

induction might be unaffected/enhanced by this experimental manipulation. On the other hand, an ASMR-Responder who prefers personal attention and simulation-like videos would be negatively affected. Whilst only ASMR-Responders as identified using the AEQ were tested in this study, an interesting addition would be to investigate the individual differences of the ASMR response using a AEQ-clustered cohort with greater stratification (i.e., Control+, Control-, ASMR-Strong, ASMR-Weak). For example, it would be interesting to see whether the Control + cohort, who find ASMR stimuli relaxing with no tingling sensations, exhibit a similar Relaxed profile to ASMR-Responders given the same self-reported state.

This study builds and expands on prior work by Fredborg and colleagues in several ways (2021). Firstly, data from a larger sample size of ASMR-Responders have been collected. Secondly, a novel control stimuli design has been tested, whereby the temporal continuity of the ASMR video has been scrambled to form the control video. We aimed to maintain all low-level features of the ASMR video, but violate the expectancy of the familiarity of the video. Thirdly, research into idiosyncratic sensory experiences such as chills often uses individualised stimuli to maximise the likelihood of a (strong) experience in experimental settings (e.g., Mori & Iwanaga, 2017). Given the control video stimuli design mentioned above, we used personalised ASMR videos to maximise ASMR intensity and likelihood with corresponding personalised control videos. In addition, our study was entirely exploratory, and thus relied on nonparametric data-driven clustering in the sensor-space order to extract meaningful results. In this way, experimenter-introduced bias can be eliminated, where no prior data in the EEG field could otherwise inform the analysis. These results from the sensor space then informed further cluster tests in the source space, thereby estimating the origin of particular oscillatory signals identified in the previous step. Moreover, our methodological design allows for inferences to be made regarding a potential decay effect of ASMR anecdotally reported previously (Barratt & Davis, 2015). Finally, our study takes ASMR-Responder identification one step further by using a new data-driven tool relying on an unsupervised machine learning algorithm, the ASMR-Experience Questionnaire (Swart et al., 2021).

There are some limitations to this study. Firstly, individualised ASMR stimuli were used to maximise the likelihood of ASMR induction. The relative drawback of this approach is the non-standardised stimuli which may have affected the results and interpretations. For example, some individualised ASMR stimuli contained whispering sounds, whilst others did not. Consequently, some neural differences seen may be a result of the different processing required for such stimuli. Secondly, as indicated in the prior EEG study, several participants indicated that the EEG equipment setup (and the required personal attention) induced ASMR itself. Since we have shown there are indeed decay effects, these confounds might be present in our data. Thirdly, a template headmodel was applied to all datasets, and thus the source localisations could bear minor inaccuracies. For example, one assumption of using a template brain is that the participants' brain anatomy are "normal". This assumption may, thus, bias the differences identified between certain brain regions. The error (e.g., spectral leakage) present in this identification can be minimised using individualised anatomical images. However, consistent electrode cap placements should minimise these inaccuracies. Future work could include a follow-up MRI study capturing the anatomical images of the participant cohort reported here. In addition, future work using simultaneous EEG and novel near-silent fMRI adaptations such as Looping Star fMRI would help confirm identified regions whilst minimising the loud environment typically associated with an MRI scanner (Dionisio-Parra, Wiesinger, Sämann, Czisch, & Solana, 2020; Lochte et al., 2018). This technique would be well suited to capture with high accuracy and precision both temporal and spatial features of the ASMR experience in real-time. A clearer picture will be seen if a study design incorporates effective control stimuli and a control participant group. Finally, whilst no differences were found in tingle duration between experimental and control videos, the scrambling effect may have influenced the results from the combined dataset.

Altogether, we showed the robust changes in the patterns of dynamical brain oscillations associated with an ASMR tingling experience and identified its underlying cortical network. Further, we demonstrated the long-lasting effects of ASMR across a wide range of brain regions and oscillatory powers, including evidence for prolonged relaxation, offering potential neurophysiological support for the speculative therapeutic claim of ASMR.

Credit author statement

Thomas Swart: Conceptualization, Data curation, Funding acquisition, Investigation, Methodology, Software, Formal analysis, Writing - Original Draft, Visualization, Writing - Review & Editing. **Michael Banissy:** Conceptualization, Funding acquisition, Writing - Review & Editing, Supervision. **Thomas Hein:** Software, Formal analysis, Writing - Original Draft, Writing - Review & Editing. Ricardo Bruña: Software, Data Curation, Formal analysis, Writing - Review & Editing.: **Ernesto Pereda:** Writing - Review & Editing, Validation.: **Joydeep Bhattacharya:** Conceptualization, Methodology, Project administration, Resources, Supervision, Validation, Writing-Reviewing and Editing.

Open practices

The study in this article earned an Open Data and Open Materials badges for transparent practices. Data and Materials for this study can be found at: https://osf.io/dg3y5/?view_only=9e7276fd3b2e44a6a3ca5943cba610fe.

Additional information

No part of the study was pre-registered prior to the research being conducted.

Funding

This research was supported by a grant from the BIAL Foundation [#71/18].

Declaration of competing interest

All authors declare no conflict of interest.

Supplementary data

Supplementary data to this article can be found online at https://doi.org/10.1016/j.cortex.2022.01.004.

REFERENCES

Arnal, L. H., & Giraud, A.-L. (2012). Cortical oscillations and sensory predictions. *Trends in Cognitive Sciences, 16*(7), 390–398.

Barratt, E. L., & Davis, N. J. (2015). Autonomous sensory meridian response (ASMR): A flow-like mental state. *Peerj, 3*, Article e851. https://doi.org/10.7717/peerj.851

Barratt, E. L., Spence, C., & Davis, N. J. (2017). Sensory determinants of the autonomous sensory meridian response (ASMR): Understanding the triggers. *Peerj, 5*, Article e3846. https://doi.org/10.7717/peerj.3846

Başar, E., Başar-Eroğlu, C., Karakaş, S., & Schürmann, M. (1999). Are cognitive processes manifested in event-related gamma, alpha, theta and delta oscillations in the EEG? *Neuroscience Letters, 259*(3), 165–168. https://doi.org/10.1016/S0304-3940(98)00934-3

Benjamini, Y., Krieger, A. M., & Yekutieli, D. (2006). Adaptive linear step-up procedures that control the false discovery rate. *Biometrika, 93*(3), 491–507. https://doi.org/10.1093/biomet/93.3.491

Chandrasekaran, C., & Ghazanfar, A. A. (2009). Different neural frequency bands integrate faces and voices differently in the superior temporal sulcus. *Journal of Neurophysiology, 101*(2), 773–788. https://doi.org/10.1152/jn.90843.2008

Chen, Y.-H., Edgar, J. C., Holroyd, T., Dammers, J., Thönneßen, H., Roberts, T. P. L., & Mathiak, K. (2010). Neuromagnetic oscillations to emotional faces and prosody. *European Journal of Neuroscience, 31*(10), 1818–1827. https://doi.org/10.1111/j.1460-9568.2010.07203.x

Cheyne, D., Gaetz, W., Garnero, L., Lachaux, J.-P., Ducorps, A., Schwartz, D., & Varela, F. J. (2003). Neuromagnetic imaging of cortical oscillations accompanying tactile stimulation. *Cancer Biotherapy & Radiopharmaceuticals, 17*(3), 599–611. https://doi.org/10.1016/S0926-6410(03)00173-3

Clark, J. M. (1996). Contributions of inhibitory mechanisms to unified theory in neuroscience and psychology. *Brain and Cognition, 30*(1), 127–152.

Cooper, N. R., Burgess, A. P., Croft, R. J., & Gruzelier, J. H. (2006). Investigating evoked and induced electroencephalogram activity in task-related alpha power increases during an internally directed attention task. *Neuroreport, 17*(2), 205–208.

Craig, A. D., & Craig, A. D. (2009). How do you feel—now? The anterior insula and human awareness. *Nature Reviews Neuroscience, 10*(1).

Delorme, A., & Makeig, S. (2004). Eeglab: An open source toolbox for analysis of single-trial EEG dynamics including independent component analysis. *Journal of Neuroscience Methods, 134*(1), 9–21. https://doi.org/10.1016/j.jneumeth.2003.10.009

Dionisio-Parra, B., Wiesinger, F., Sämann, P. G., Czisch, M., & Solana, A. B. (2020). Looping star fMRI in cognitive tasks and resting state. *Journal of Magnetic Resonance Imaging, 52*(3), 739–751.

Engel, A. K., & Fries, P. (2010). Beta-band oscillations—signalling the status quo? *Current opinion in neurobiology, 20*(2), 156–165.

Eulitz, C., & Obleser, J. (2007). Perception of acoustically complex phonological features in vowels is reflected in the induced brain-magnetic activity. *Behavioral and Brain Functions: BBF, 3*(1), 26. https://doi.org/10.1186/1744-9081-3-26

Foxe, J. J., & Snyder, A. C. (2011). The role of alpha-band brain oscillations as a sensory suppression mechanism during selective attention. *Frontiers in psychology, 2*, 154.

Fredborg, B. K., Champagne-Jorgensen, K., Desroches, A. S., & Smith, S. D. (2021). An electroencephalographic examination of the autonomous sensory meridian response (ASMR). *Consciousness and Cognition, 87*, 103053. https://doi.org/10.1016/j.concog.2020.103053

Fredborg, B. K., Clark, J., & Smith, S. D. (2017). An examination of personality traits associated with autonomous sensory meridian response (ASMR). *Frontiers in Psychology, 8*, 247. https://doi.org/10.3389/fpsyg.2017.00247

Fredborg, B. K., Clark, J. M., & Smith, S. D. (2018). Mindfulness and autonomous sensory meridian response (ASMR). *Peerj, 6*, e5414. https://doi.org/10.7717/peerj.5414

Frühholz, S., Trost, W., & Grandjean, D. (2016). Whispering—the hidden side of auditory communication. *Neuroimage, 142*, 602–612. https://doi.org/10.1016/j.neuroimage.2016.08.023

Gramfort, A., Papadopoulo, T., Olivi, E., & Clerc, M. (2010). OpenMEEG: Opensource software for quasistatic bioelectromagnetics. *Biomedical Engineering Online, 9*(1), 45. https://doi.org/10.1186/1475-925X-9-45

Gross, J., Kujala, J., Hämäläinen, M., Timmermann, L., Schnitzler, A., & Salmelin, R. (2001). Dynamic imaging of coherent sources: Studying neural interactions in the human brain. *Proceedings of the National Academy of Sciences, 98*(2), 694–699. https://doi.org/10.1073/pnas.98.2.694

Hammond, D. C. (2003). The effects of caffeine on the brain: A review. *Journal of Neurotherapy, 7*(2), 79–89.

Huang, Y., Parra, L. C., & Haufe, S. (2016). The New York Head—a precise standardised volume conductor model for EEG source localisation and tES targeting. *Neuroimage, 140*, 150–162. https://doi.org/10.1016/j.neuroimage.2015.12.019

Jann, K., Kottlow, M., Dierks, T., Boesch, C., & Koenig, T. (2010). Topographic electrophysiological signatures of fMRI resting state networks. *Plos One, 5*(9). https://doi.org/10.1371/journal.pone.0012945

Jensen, O., Gelfand, J., Kounios, J., & Lisman, J. E. (2002). Oscillations in the alpha band (9–12 Hz) increase with memory load during retention in a short-term memory task. *Cerebral Cortex, 12*(8), 877–882.

Jensen, O., & Mazaheri, A. (2010). Shaping functional architecture by oscillatory alpha activity: Gating by inhibition. *Frontiers in Human Neuroscience, 4*, 186.

Kelly, S. P., Lalor, E. C., Reilly, R. B., & Foxe, J. J. (2006). Increases in alpha oscillatory power reflect an active retinotopic mechanism for distracter suppression during sustained visuospatial attention. *Journal of neurophysiology, 95*(6), 3844–3851.

Klimesch, W., Sauseng, P., & Hanslmayr, S. (2007). EEG alpha oscillations: The inhibition–timing hypothesis. *Brain Research Reviews, 53*(1), 63–88. https://doi.org/10.1016/j.brainresrev.2006.06.003

Knott, V., Cosgrove, M., Villeneuve, C., Fisher, D., Millar, A., & McIntosh, J. (2008). EEG correlates of imagery-induced cigarette craving in male and female smokers. *Addictive Behaviors, 33*(4), 616–621.

Knyazev, G. G. (2007). Motivation, emotion, and their inhibitory control mirrored in brain oscillations. *Neuroscience and Biobehavioral Reviews, 31*(3), 377–395. https://doi.org/10.1016/j.neubiorev.2006.10.004

Knyazev, G. G., Slobodskoj-Plusnin, J. Y., Bocharov, A. V., & Pylkova, L. V. (2011). The default mode network and EEG alpha oscillations: An independent component analysis. *Brain Research, 1402*, 67–79. https://doi.org/10.1016/j.brainres.2011.05.052

Kothe, C. A., & Makeig, S. (2013). Bcilab: A platform for brain–computer interface development. *Journal of Neural Engineering, 10*(5), Article 056014. https://doi.org/10.1088/1741-2560/10/5/056014

Kovacevich, A., & Huron, D. (2019). Two studies of autonomous sensory meridian response (ASMR): The relationship between ASMR and music-induced frisson. *[Environmental Microbiology Reports Electronic Resource], 13*(1–2), 39. https://doi.org/10.18061/emr.v13i1-2.6012

Lochte, B. C., Guillory, S. A., Richard, C. A. H., & Kelley, W. M. (2018). An fMRI investigation of the neural correlates underlying the autonomous sensory meridian response (ASMR). *Bioimpacts, 8*(4), 295–304. https://doi.org/10.15171/bi.2018.32

Magosso, E., De Crescenzio, F., Ricci, G., Piastra, S., & Ursino, M. (2019). *Eeg alpha power is modulated by attentional changes during cognitive tasks and virtual reality immersion.* Computational Intelligence and Neuroscience, 2019.

Maris, E., & Oostenveld, R. (2007). Nonparametric statistical testing of EEG- and MEG-data. *Journal of Neuroscience Methods, 164*(1), 177–190. https://doi.org/10.1016/j.jneumeth.2007.03.024

Matsuoka, T., Shimode, T., Ota, T., & Matsuo, K. (2021). Event-related alpha-band power changes during self-reflection and working memory tasks in healthy individuals. *Frontiers in Human Neuroscience, 14*. https://doi.org/10.3389/fnhum.2020.570279

Mccraty, R., & Shaffer, F. (2015). Heart rate variability: New perspectives on physiological mechanisms, assessment of self-regulatory capacity, and health risk. *Global Advances in Health and Medicine, 4*(1), 46–61. https://doi.org/10.7453/gahmj.2014.073

Mori, K., & Iwanaga, M. (2017). Two types of peak emotional responses to music: The psychophysiology of chills and tears. *Scientific Reports, 7*(1), 46063. https://doi.org/10.1038/srep46063

Mu, Y., & Han, S. (2010). Neural oscillations involved in self-referential processing. *Neuroimage, 53*(2), 757–768.

Mullen, T. R., Kothe, C. A. E., Chi, Y. M., Ojeda, A., Kerth, T., Makeig, S., Jung, T.-P., & Cauwenberghs, G. (2015). Real-time neuroimaging and cognitive monitoring using wearable dry EEG. *IEEE Transactions on Bio-Medical Engineering, 62*(11), 2553–2567. https://doi.org/10.1109/TBME.2015.2481482

Niedermeyer, E. (1999). The normal EEG of the waking adult. In E Niedermeyer, & F Lopes da Silva (Eds.), *Electroencephalography: Basic principles, Clinical Applications and Related Fields* (4th ed., pp. 149–173). Philadelphia, PA: Williams and Wilkins.

Oliveri, M., Babiloni, C., Filippi, M. M., Caltagirone, C., Babiloni, F., Cicinelli, P., Traversa, R., Palmieri, M. G., & Rossini, P. M. (2003). Influence of the supplementary motor area on primary motor cortex excitability during movements triggered by neutral or emotionally unpleasant visual cues. *Experimental Brain Research, 149*(2), 214–221.

Oostenveld, R., Fries, P., Maris, E., & Schoffelen, J.-M. (2011). FieldTrip: Open source software for advanced analysis of MEG, EEG, and invasive electrophysiological data. *Computational Intelligence and Neuroscience*, 1–9. https://doi.org/10.1155/2011/156869, 2011.

Poerio, G. L., Blakey, E., Hostler, T. J., & Veltri, T. (2018). More than a feeling: {Autonomous} sensory meridian response (asmr) is characterised by reliable changes in affect and physiology. *Plos One, 13*(6). https://www.scopus.com/inward/record.uri?eid.=2-s2.0-85048815069&doi=10.1371%2fjournal.pone.0196645&partnerID=40&md5=e73f4bf8345e26b62948000f103f743c.

Sanz-Martin, A., Guevara, M.Á., Amezcua, C., Santana, G., & Hernández-González, M. (2011). Effects of red wine on the electrical activity and functional coupling between prefrontal–parietal cortices in young men. *Appetite, 57*(1), 84–93.

Schultz, W. (2000). Multiple reward signals in the brain. *Nature Reviews Neuroscience, 1*(3), 199–207.

Senkowski, D. (2005). Oscillatory beta activity predicts response speed during a multisensory audiovisual reaction time task: A high-density electrical mapping study. *Cerebral Cortex, 16*(11), 1556–1565. https://doi.org/10.1093/cercor/bhj091

Smith, S. D., Fredborg, B. K., & Kornelsen, J. (2017). An examination of the default mode network in individuals with autonomous sensory meridian response ([ASMR]). *Social Neuroscience, 12*(4), 361–365.

Smith, S. D., Fredborg, B. K., & Kornelsen, J. (2019a). Atypical functional connectivity associated with autonomous sensory meridian response: An examination of five resting-state networks. *Brain Connectivity, 9*(6), 508–518.

Smith, S. D., Fredborg, B. K., & Kornelsen, J. (2019b). A functional magnetic resonance imaging investigation of the autonomous sensory meridian response. *Peerj, 7*, Article e7122. https://doi.org/10.7717/peerj.7122

Smith, S. D., Fredborg, B. K., & Kornelsen, J. (2020). Functional connectivity associated with five different categories of Autonomous Sensory Meridian Response (ASMR) triggers. *Consciousness and Cognition, 85*, 103021.

Spitzer, B., & Haegens, S. (2017). Beyond the status quo: a role for beta oscillations in endogenous content (re) activation. *Eneuro, 4*(4).

Swart, T. R., Bowling, N. C., & Banissy, M. J. (2021). ASMR-experience Questionnaire (AEQ): A data-driven step towards accurately classifying ASMR responders. *British Journal of Psychology, 113*.

Symons, A. E., El-Deredy, W., Schwartze, M., & Kotz, S. A. (2016). The functional role of neural oscillations in non-verbal emotional communication. *Frontiers in Human Neuroscience, 10*. https://doi.org/10.3389/fnhum.2016.00239

Tallon-Baudry, C., Bertrand, O., Hénaff, M.-A., Isnard, J., & Fischer, C. (2005). Attention modulates gamma-band oscillations differently in the human lateral occipital cortex and fusiform gyrus. *Cerebral Cortex, 15*(5), 654–662. https://doi.org/10.1093/cercor/bhh167

Trochidis, K., & Bigand, E. (2012). *EEG-based emotion perception during music listening* (Vol. 5).

Tzourio-Mazoyer, N., Landeau, B., Papathanassiou, D., Crivello, F., Etard, O., Delcroix, N., Mazoyer, B., & Joliot, M. (2002). Automated anatomical labeling of activations in SPM using a macroscopic anatomical parcellation of the MNI MRI single-subject brain. *Neuroimage, 15*(1), 273–289. https://doi.org/10.1006/nimg.2001.0978

Villena-González, M., Palacios-García, I., Rodríguez, E., & López, V. (2018). Beta oscillations distinguish between two forms of mental imagery while gamma and theta activity reflects auditory attention. *Frontiers in Human Neuroscience, 12*, 389.

Vollmer, M. (2015). A robust, simple and reliable measure of heart rate variability using relative RR intervals. In *2015 computing in cardiology conference (CinC)*, 609–612. https://doi.org/10.1109/CIC.2015.7410984

Vollmer, M. (2019). *HRVTool – an open-source matlab toolbox for analyzing heart rate variability*. 2019 Computing in cardiology (CinC). https://doi.org/10.23919/CinC49843.2019.9005745. Page 1-Page 4.

Worden, M. S., Foxe, J. J., Wang, N., & Simpson, G. V. (2000). Anticipatory biasing of visuospatial attention indexed by retinotopically specific α-bank electroencephalography increases over occipital cortex. *Journal of Neuroscience, 20*(6), RC63. RC63.